Molecular Modeling and Simulation of Water near Model Micelles: Diffusion, Rotational Relaxation and Structure at the Hydration Interface

Fabio Sterpone

Commissariat à l'Energie Atomique, DSV-DBJC−SBFM, Centre d'Études, Saclay, 91191 Gif-sur-Yvette Cedex, France and Department of Chemistry and Biochemistry, University of Texas at Austin, 1 University Station A5300, Austin, Texas 78712

Gino Marchetti

Commissariat à l'Energie Atomique, DSV-DBJC−SBFM, Centre d'Études, Saclay, 91191 Gif-sur-Yvette Cedex, France

Carlo Pierleoni

INFM CRS−SOFT and Dipartimento di Fisica, Università dell'Aquila, via Vetoio, I-67010 L'Aquila, Italy

Massimo Marchi*

Commissariat à l'Energie Atomique, DSV-DBJC−SBFM, Centre d'Études, Saclay, 91191 Gif-sur-Yvette Cedex, France

Received: December 13, 2005; In Final Form: April 20, 2006

This paper reports on molecular dynamics simulations of two hydrated micelles composed of $C_{12}E_6$ and LDAO surfactants. The simulations results provide a quantitative picture of the dynamics of the hydration water at the water/micelle interface. Both the residence time of water near the micelle surface and its retardation with respect to the bulk have been estimated. It is found that the water dynamics is radically different for the two micellar systems and depends on the physical nature of the micelle surface in contact with water. For $C_{12}E_6$ this interface is thicker and presents a stronger hydrophilic character than that of LDAO. Thus, in $C_{12}E_6$, surface water dynamics is 1−2 orders of magnitude slower than that of bulk water, compared with only 18% for the LDAO system. The simulations have also revealed the nature of the rotational landscape experienced by water at the micellar surface: In the $C_{12}E_6$ micelle water rotation occurs in a highly anisotropic space due to confinement of waters at the interface; in LDAO the rotational landscape is instead isotropic. These findings clearly indicate that the slowdown of interfacial water relaxation near complex micelles depends, case by case, on the structural properties of the interface itself, such as the ratio between hydrophobic/hydrophilic exposed regions and on the interface thickness and topography.

I. Introduction

The behavior of water in the proximity of biological surfaces is crucial in many processes such as enzymatic activity, molecular recognition, and protein folding. Recent experiments and theoretical efforts focused on characterizing the first hydration shell of biomolecules with particular attention to the structure and dynamics of water at the interface. In this way, the dynamic behavior of water around folded and partially unfolded proteins,[1−4] DNA strands,[5] and direct and reversed micelles[6−8] has been investigated. On the basis of dielectric measurements, NMR dispersion (NMRD), solvation dynamics techniques, quasi elastic neutron scattering (QENS), and molecular dynamics simulations (MD), it was observed that water dynamics is retarded with respect to the bulk, showing peculiar features such as dispersive diffusion[2,9] and slow orientational relaxation. The origin of the water slow-down near a biological surface is not yet fully understood. For example, it is still not clear if the dispersive diffusion of surface water arises from the geometrical disorder (*à voir* its roughness) or from energetic disorder, due to the alternating hydrophilic/hydrophobic patches.[10] The magnitude of the water retardation and the ratio between the time scales of surface and bulk water is also questioned, whereas time-resolved spectroscopy estimates water retardation as 1 to 3 orders of magnitude,[4] NMRD detects a smaller retardation, <1 order of magnitude.[11,12]

This paper is concerned with the structural and dynamic properties of hydration water near micellar aggregates. Micelles in water solutions represent an interesting prototype of biological surface. First, at the interface with water, the hydrophilic groups alternate with the unscreened hydrophobic parts of the micelle forming detergent molecules creating a mixture of water binding and water repelling sites. Second, the relative occurrence of hydrophilic and hydrophobic patches on the surface and the chemical and physical character of both regions can be changed at will, by modifying the head and tail of the detergents.

In the past, experiments have been devised to measure the solvation dynamics of a chemical probe residing at the micellar interface. Systems investigated with this technique are the titron

* Corresponding author.

10.1021/jp057282f CCC: $33.50
Published on Web 05/24/2006

X-100 (TX-100), cetyl-trimethylammonium-bromide (CTAB), and sodium-dodecyl-sulfate (SDS).[1,6,13] It was found that the solvation relaxation decays with two time scales: A fast one with a characteristic time in the order of a few ps, thus comparable with the relaxation time of bulk water ($\simeq$1 ps), and a slow one with characteristic time in the range of 50−1000 ps. For the TX-100 system in particular, the relative weight between the fast and the slow component was found close to 1,[1] whereas for other systems, it is expected to be larger.[14] This ratio appears to depend on the extension and polarity of the surfactant hydrophilic groups and on its interfacial structure.[7] The hydration state of the interface has also been demonstrated to play an important role. Indeed, water solvation was found to be slower at drier interfaces (see, for example, the results for the ionic micelles CTAB and SDS[6,13] and for the nonionic micelles TX-100 and Brij-35[15]).

Recently, QENS study of SDS and NMR measurements of dodecyl-trimethyl-ammonium-bromide (DTAB) and of ethoxylated nonyl phenols (9NX) micellar solutions detected a net slowdown of the water diffusion for all the examined systems.[16] In the case of 9NX, the micelle structure at the interface was modified by increasing the length of the hydrophilic part. It was found that when the number of ethoxy groups was augmented from 10 units up to 40, the mean water diffusion coefficient of the solution, $\bar{D}_w$, decreased about 14%. This was interpreted as due to the increase of the amount of water trapped at the interface, hydrogen bound to the solute.

To elucidate the molecular origin of the slow water relaxation and diffusion, MD has also been used to study the water dynamics near a micellar interface.[7,17−19] The decay of the survival probability of the H-bonds formed between a water molecule and a hydrophilic group in a micellar system of cesium pentadecafluorooctanate (CsPFO) has been found to be 13 times slower than that of a water−water H-bond in the bulk.[19] For this system and for a SDS micelle, the dipolar relaxation of water molecules near the micellar surface was estimated at 2 order of magnitude slower than that in the corresponding bulk solution.[17,20] Sub-diffusive dynamics, or dispersive diffusion, was also observed for water molecules less than 6 Å from the micellar surface, which also experienced residence times 4 times larger than those observed in the bulk.[18] Experiments as well as simulation studies have shown that the water behavior at the interface is critically influenced by the electrostatic nature of the interaction between the hydrophilic groups and water within a few layers from the interface. Nonetheless, there are yet no indications that a critical size, concentration, or distribution of the hydrophilic groups at the interface exists, which leads to the anomalous dynamic behavior of water.

Our investigation addresses the issue of how water dynamics is affected by large changes in the hydrophilic nature of the micellar interface. Two topical micelles characterized by a very different composition of their interface have been studied. Our first system is constituted by a spherical micelle of $C_{12}E_6$ in water. We present here a new analysis of the trajectories previously generated for studying the temperature dehydration in such a micellar solution.[21] $C_{12}E_6$ is a surfactant belonging to the family of olygoethileneoxyde, composed of a hydrocarbon tail C_{12}, CH_3-$(CH_2)_{11}$, and of a hydrophilic moiety of 6 E units, $(O-CH_2-CH_2)_6$, ending with a group OH. According to a previous study,[21] the $C_{12}E_6$ spherical micelle has an extended interfacial region in which the long hydrophilic moieties bind and trap water molecules. Our second system is constituted by a hydrated oblate micelle of lauryl dimethyl amino oxide (LDAO). To our knowledge it is the first time that a MD simulation of this micelle has been carried out. LDAO is a detergent with a hydrophobic tail C_{12} which ends with a small hydrophilic group $NO-(CH_3)_2$ whose polar site (NO) is screened by the methyl groups CH_3. As a consequence, the thickness of the interfacial region is much smaller than that found in $C_{12}E_6$, whereas the accessibility to the binding sites is reduced. In a previous study of the $C_{12}E_6$ spherical micelle,[21] some of us have shown that, upon rise in the temperature, dehydration at the interface is accompanied by a spatial redistribution of the hydrophilic units. Hence, the study of this system at low ($T = 10$ °C) and high ($T = 45$ °C) allows us to monitor the relation between the interface's structure and the water dynamics

These two micellar systems allow us to investigate the effect of both electrostatic interactions and spatial confinement of water in the interface. The latter aspect particularly affects the estimates of water retardation from NMRD measurements, which relies on the assumption that water rotational and translational diffusion are both only rate limited by hydrogen bond breaking and making. When spatial confinement is important, such assumption is no longer acceptable.

Anticipating our main results, we observe a strong effect of the micellar interface properties on the hydration dynamics. For the $C_{12}E_6$ micelle water dynamics has a slow component in the order of 50−100 ps, depending on the temperature, whereas for the LDAO system, the temporal correlations have bulklike relaxation times. Moreover, the dynamics of water is sub-diffusive in the interface of $C_{12}E_6$ micelle, whereas it is close to the Brownian regime in the LDAO micellar surface. Indeed, we find that the rotation of the water molecules on the open surface of LDAO occurs in a quasi isotropic space. On the contrary a strong deviation from the isotropic regime is observed for water at the $C_{12}E_6$ micelle interface.

The paper is organized as follows: In Section II, we describe the systems composition, the simulation protocols, and the time correlation functions employed in the study of the dynamics of hydration. Section III presents our findings for the structural properties of the micelle/water interface. In Section IV, we present and discuss our results for the survival probability of the micelle−water bond. Rotational relaxation and translational diffusion are discussed in Sections V and VI, respectively. Our conclusions are reported in the final section.

II. Methods

A. **Systems and Molecular Dynamics Simulations.** *1. $C_{12}E_6$.* This first system consisted of a micelle formed by 45 $C_{12}E_6$ monomers and 8448 water molecules. The aggregation number of the micelle has been derived from a thermodynamic model, which predicts the optimal oil core radius (l^*) for a given surfactant and micellar shape. For a $C_{12}E_6$ spherical micelle $l^* =$ 15.4 Å and assuming the oil core density $\rho = 0.75$ g/cm^3, the aggregation number is $\simeq$ 45, see ref 22. The system was simulated in a truncated octahedral cell. This corresponds to simulate a nonorthogonal simulation cell with angular parameters $\alpha = \beta = \gamma = 109.47°$. The initial axis of our system were $a = b = c = 84$ Å. The system preparation is detailed in the Supporting Information. An all-atom force field described the interactions between the constituents of the system.[24] The simple point charge model (SPC)[25] was used for the water molecules. In this system all bond lengths were fixed at the equilibrium value by the constraints method.[26]

The $C_{12}E_6$ micelle was simulated in the NPT ensemble[28] at two temperatures, $T = 10$ °C and $T = 45$ °C, and pressure $P =$ 1 atm. Electrostatic interactions were handled by the smooth

particle mesh Ewald (SPME) technique.[27] We used an Ewald sum exponential convergence parameter α of 0.33 Å^{-1}, 60 grid points in each directions and an order $n = 4$ for the spline interpolation. Non bonded Lennard−Jones (L−J) and real space electrostatic interactions were truncated at $r_c = 12$ Å. The L−J potential was then shifted to zero and smoothed in an interval of 0.5 Å around the cutoff with a switching function ensuring the continuity of the forces. The equations of motion were integrated with a time step of $t = 1$ fs. After 100 ps of equilibration, four independent trajectories at $T = 10$ °C and eight at $T = 45$ °C were run for a total simulation time of 1.2 ns and 2 ns, respectively. The average volume of the simulation cell is $V = 2.957 \times 10^5$ Å^3 and $V = 3.038 \times 10^5$ Å^3 at $T = 10$ °C and $T = 45$ °C, respectively. Configurations have been stored each 200 fs. All the simulations of $C_{12}E_6$ were carried out using the DLPROTEIN program[29] on a Linux cluster.

2. LDAO. Our second system consisted of a micelle composed of 104 monomers of LDAO and 1629 molecules of water. This aggregation number was obtained from ref 30. As for $C_{12}E_6$, our system was placed in simulation cell with truncated octahedron periodicity, with nonorthogonal axis $a = b = c =$ 79.5 Å. The all atom CHARMM22[31] force field described the interactions between the constituents of the system, while the charges distributions on the polar heads are derived from ab initio calculations by Ceccarelli et al.[32] (see the Supporting Information for details of the force field). Consistently, with the CHARMM22 force field protocol, the TIP3P[33] model was used to describe the water molecules. As for our previous system all bond lengths involving hydrogen atoms were fixed by rigid constraints.[26]

The LDAO micelle was simulated in the NPT ensemble at temperature $T = 27$ °C, and pressure $P = 1$ atm using the technique described in ref 34. The barostat and thermostat masses were chosen to obtain characteristic oscillatory frequency of approximately 30 and 40 cm^{-1}, respectively. A five time-step r-RESPA[34] integration scheme with a Liouvillean separation in three nonbonded shells was used to propagate the system in time. The SPME scheme was also used to handle electrostatic interactions with $\alpha = 0.43$ Å^{-1}, 80 grid points in each direction and $n = 5$ for spline interpolation. After an equilibration period 100 ps long, the system was run for 3 ns, storing configurations each 240 fs. The simulation of the LDAO micelle was carried out using the parallel version of ORAC.[35,36] All the parameters of the integration algorithm, time step, and cutoffs, are the same as those in ref 34.

B. Analysis of the Trajectories. The dynamics of hydration was investigated by computing the survival probability, the rotational relaxation, and translational diffusion of the water molecules of the first hydration shell. A water molecule is considered to be in the first hydration shell if its Voronoi polyhedron[37] shares at least one face with an atom of the micellar aggregate. All the Voronoi calculations were carried out using the technique described in ref 38.

1. Survival Probability. As defined in ref 39, the survival probability, $N_w(t)$, gives the probability that a water molecule is in contact with the micelle for a time t. To obtain $N_w(t)$, we compute the conditional probability $P_j(t_n,t)$ for each jth water molecule of the system and then average it over the length of the run:

$$N_w(t) = \frac{1}{N_t}\sum_{n=1}^{N_t}\sum_j P_j(t_n, t) \tag{1}$$

Here, $P_j(t_n,t)$ takes the values of 1 if the jth water is in contact to any of the surfactant molecules between times t_n and t_n+t, and zero if otherwise. N_t is the number of the simulation time frames of length t.

We remark that $N_w(t)$ takes important meanings for $t = 0$ and for the t equal to the length of the simulation, $t = t_{sim}$. Indeed, $N_w(0)$ is the average number of hydration water, whereas $N_w(t_{sim})$ correspond to the number of waters permanently attached to the solute, in our case the micelle.

For both our systems, we discerned two time scales after fitting the survival probability with a linear combination of a stretched exponential and an exponential function, i.e.,

$$N_w(t) \simeq n^s \exp\left(-\left(\frac{t}{\tau^s}\right)^\gamma\right) + n_1 \exp\left(-\frac{t}{\tau_1}\right) \tag{2}$$

Thus, we take $\tau_w = \tau_1$ as the water residence time of the exponential part, whereas for the stretched exponential part we define τ_w as the average relaxation time, or

$$< \tau^s > = \int_0^\infty e^{-(t/\tau_s)^\gamma} dt = \frac{\tau^s}{\gamma}\Gamma\left(\frac{1}{\gamma}\right) \tag{3}$$

where Γ is the Euler gamma function.

2. Rotational Relaxation and Translational Diffusion. To compare our simulation results with NMRD experiments, τ_w needs to be estimated in a different manner.[9] Indeed, NMRD can readily obtain the characteristic time of rotational relaxation, τ_R. If it is assumed that rotation and translation of water molecules are rate limited by hydrogen bonds disruption, then τ_R is a good estimate of τ_w.

To investigate the rotational relaxation of water in the hydration shell, we computed the first and second rank dipole−dipole correlation:

$$P_1(t) = < \cos\theta(t) > \tag{4}$$

$$P_2(t) = <\frac{3}{2}\cos^2\theta(t) - \frac{1}{2}> \tag{5}$$

where $\theta(t)$ is the angle between the water dipole of the same molecule at time τ and $\tau + t$ ad $\langle..\rangle$ stands for statistical average.[9] The comparison of $P_1(t)$ and $P_2(t)$ computed for the hydration waters with a simple kinetic relaxation models makes it possible to estimate their characteristic times, τ_R^1 and τ_R^2.

In general, NMRD experiments can make direct estimates of τ_R^2 and obtain τ_R^1 from the assumption that the rotational diffusion of hydration waters is isotropic, which gives

$$r = \frac{\tau_R^{\,1}}{\tau_R^{\,2}} \simeq 3 \tag{6}$$

In past simulations, we have shown that, at least for globular proteins, this relation is satisfied, and found for a protein such as lysozyme $r = 2.7$.[9]

The order of magnitude of τ_w can also be estimated in MD simulations by computing the average mean square displacement of water, $< |\boldsymbol{r}(t) - \boldsymbol{r}(0)|^2 >$, as a function of time. As a rough measure of the residence time we use throughout this study the time required by a water molecule to cover a distance of 3 Å.

III. Interfacial Properties

A spherical micelle of $C_{12}E_6$ in water solution is characterized by an extended interfacial region between the segregated hydrophobic core and the bulk solvent. The oil core radius is roughly 10 Å, and the long hydrophilic tails extend 17 Å away

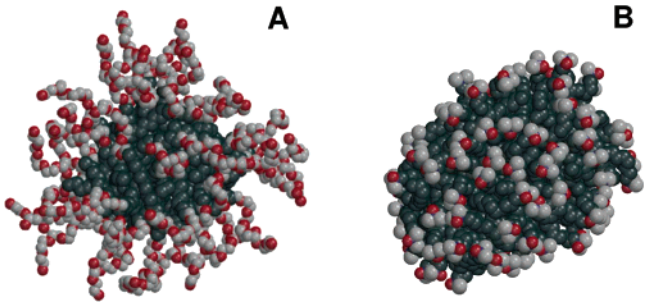

Figure 1. Pictorial view of the $C_{12}E_6$ spherical micelle (panel A) and the LDAO oblate micelle (panel B), from instantaneous conformations obtained of our MD simulations. For both panels, the hydrophobic core is colored in dark gray, the methylene groups in light gray, and the oxygen of the hydrophilic fragments in red. In both pictures water is not shown. In both the micelles large portions of the hydrophobic core are not screened to water. In $C_{12}E_6$ the hydrophilic moieties (E_6) form a complex network in which water molecules can be trapped forming several kinds of hydrogen bonds. On the contrary in the LDAO micelle, water molecules can form hydrogen bonds only with the small polar heads.

from the core surface.[21] Since a large part of the core surface directly is exposed to the solvent, the hydration water can be naturally separated in two classes: (a) molecules in contact with the oil core surface not screened by the hydrophilic fragments (almost the 20% of the hydration water); (b) molecules in contact with the hydrophilic units. Among these water molecules, a subset (about the 30% of the total hydration water) forms H-bonds with the solute, stabilizing the α-helix structure of the E_6 fragments (see refs 23, 40) or bridging E units of different monomers. In agreement with experimental data,[41] a dehydration phenomena is observed upon increasing temperature.[21] The dehydration changes the structure of the interface. Indeed, the number of water in contact with the oil core decreases of about the 8% when temperature changes from $T = 10$ °C ($N_w = 226$) to $T = 45$ °C ($N_w = 209$), and the core surface exposed to the solvent (about the 30% of the total micellar surface) decreases from $\sigma = 3000$ Å^2 ($T = 10$ °C) to $\sigma = 2821$ Å^2 ($T = 45$ °C). On the other hand, the hydration state of the hydrophilic segments is weakly affected by temperature. In addition, it turns out that the dehydration is accompanied by a different distribution of the hydrophilic units in the interface.[21]

The LDAO micelle simulated at $T = 27°$ C has an ellipsoidal shape. To describe its shape, the three semi-axis of an ellipsoids of identical mass and moment of inertia as those of the micelle can be computed (see ref 42 for details of the calculation). These are 27.9, 24.1, and 19.7 Å, which correspond to a gyration radius of $R_G = 19.2$ Å. For LDAO the hydrophobic core is largely, at least relative to the $C_{12}E_6$ micelle, exposed to water, the overall hydrocarbon surface in contact with water being almost 50% of the total exposed surface. In our simulation, the total number of hydration water is $N_w = 614$, of which 35% is in contact with the polar group (N−O). Here we consider for a water to be in contact if it share at least a facets of its Voronoi polyhedra with the group. Unlike in the $C_{12}E_6$ micelle, the polar heads are small, the Voronoi volume for the polar group is $V = 90$ Å^3, which is 20% of the total volume of the molecule. A pictorial view of the systems is given in Figure 1.

IV. Survival Probability

The survival probability is computed for the water molecules in contact with the micelles. For the $C_{12}E_6$ system the averaged functions are plotted in panel A of Figure 2 for both the investigated temperatures. The solid lines represent the fitting

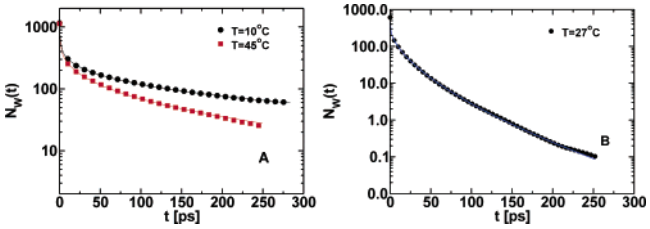

Figure 2. Panel A: Survival probability for hydration shell waters of the $C_{12}E_6$ micelle at temperature $T = 10$ °C (black circles) and $T = 45$ °C (red squares). Panel B reports the computed survival probability (black circles) for LDAO at $T = 27$ °C. In both panels, the solid lines show the fit performed with the function $n^s \cdot \exp(-(x/\tau^s)^\gamma) + n_1 \cdot \exp(-x/\tau_1)$.

TABLE 1: The Residence Times of the Hydration Waters[a]

	survival Probability				
water/micelle	τ_1(ps)	n_1	$<\tau^s>$(ps)	n^s	γ
$C_{12}E_6$ 10°C	1.5	319.1	106.6	851.0	0.28
$C_{12}E_6$ 45°C	1.0	362.5	40.6	767.3	0.35
LDAO 27°C	0.43	278.0	11.0	332.1	0.6
water/oil	τ_1(ps)	n_1	$<\tau^s>$(ps)	n^s	γ
$C_{12}E_6$ 10°C	3.1	152	50	43.2	1
$C_{12}E_6$ 45°C	2.1	146	29	43.9	1
LDAO 27°C			0.94	540.0	-

[a] computed by fitting the survival probability $N_w(t)$ with one stretched exponential ($\tau^s$and n^s) and one exponential (τ_1 and n_1). For water molecule in contact with the oil core we used a double exponential eunctions in the case of $C_{12}E_6$ and one single stretched exponential in the case of LDAO.

functions by which we extracted the temporal scales of the water−micelle contact (see Table 1). The fast relaxation is described by an exponential decay with characteristic time $\tau_1 = 1.5$ ps ($T = 10$ °C) and $\tau_1 = 1$ ps ($T = 45$ °C).

As observed for a protein system,[43] these short residence times are related to the dynamics of escape from the hydration shell to the bulk for unbound water molecules. This relaxation time is strongly affected by how the hydration shell is defined.[9] We find that the slow time scale, associated to a stretched exponential decay, gives residence times in the order of 40/100 ps, depending on the temperature, $<\tau^s> = 106.6$ ps at $T = 10$ °C and $<\tau^s> = 40.6$ ps at $T = 45$ °C. Unlike the protein case, where time scales $t > 100$ ps involves only 6% of hydration water, in the $C_{12}E_6$ micelles, the majority of water molecules in contact with the micelle, ≃70%, contributes to the longer time scale. Since about 80% of waters in the hydration shell are in contact with the hydrophilic groups,[21] the longest residence-time characterizes the water molecules involved in the hydrogen bonds network formed with the hydrophilic units (≃30%),[23] or geometrically confined in between. Moreover, a finite number of water molecules remains in the hydration shell of the micelle for the total simulation time: $N_w(t_{sim}) = 60$ at $T = 10$ °C and $N_w(t_{sim}) = 25$ at $T = 45$ °C. Longer simulations are needed to explore these slower exchange dynamics. Nonetheless, it is worth nothing that at higher temperatures the confinement of water is reduced as consequence of a different distribution of the hydrophilic fragments along the interface.

To separate the contribution of the water molecules in contact with the oil core surface or with the hydrophilic units, we compute the survival probability for these two classes of waters. For water in contact with the oil core, two time scales describe the decay (see Table 1): A fast relaxation occurs within a few picoseconds, whereas a slower one, which concerns the ≃20%

TABLE 2: Parameters Obtained from the Fit of the First and Second Rank Dipolar−Dipolar Correlation Function with a Stretched Exponential[a]

	first rank		
systems	τ_R^1(ps)	γ	$< \tau_R^1 >$(ps)
$C_{12}E_6$10°C	38.7	0.39	140 (3.7)[a]
$C_{12}E_6$45°C	15.3	0.39	54.3 (2.1)[a]
LDAO 27°C	2.1	0.68	2.7 (1.9)[b]
	second rank		
systems	τ_R^2(ps)	γ	$< \tau_R^2 >$(ps)
$C_{12}E_6$10°C	9.7	0.29	105.0 (1.24)
$C_{12}E_6$45°C	3.4	0.27	46.1 (0.69)
LDAO 27°C	0.59	0.66	0.74 (0.64)

[a] We provide the stretched exponential parameters and the average relaxation time for each case. On the third column in brackets we report the averaged relaxation time for a bulk solution of water at same thermodynamics conditions of the micellar solutions and for their water models, SPC for $C_{12}E_6$ and TIP3P for LDAO. For pure water, the first rank relaxation time is computed from the second rank time employing the isotropic model relation $< \tau_R^1 > = 3 < \tau_R^2 >$.

of these water molecules, gives a characteristic time of $\tau_2 = 50$ ps at $T = 10°$ C and $\tau_2 = 29$ ps at $T = 45$ °C.

The survival probability computed in the LDAO system is plotted in panel B of Figure 2. The same type of function used for the $C_{12}E_6$ micelle fits the correlation function as shown by the solid line curve in the plot. Two time scales for the water dynamics in the hydration shell are then found associated to characteristic times $\tau_1 = 0.43$ ps and $< \tau^s > = 11$ ps. Thus, in this system, waters exchange with the bulk with times drastically shorter, <20 ps, than in the $C_{12}E_6$ system.

As done previously for the $C_{12}E_6$ we have studied the hydration dynamics near the hydrophobic part of the surface. The survival probability in this case decays quickly, $\tau \simeq 0.94$ ps and unlike in the $C_{12}E_6$ micelle no slow component is detected.

The slow component observed only in the $C_{12}E_6$ micelle can be understood in terms of geometrical confinement of water near the hydrophobic patches of the surface, surrounded by the hydrophilic units.[21] Also, water molecules in contact with the hydrophobic surface patches have a high probability of forming hydrogen bonds with the oxygens of the innermost E unit.

The stretched decay of the survival probability is related to the presence of a manyfold of the decay processes, thus the γ exponent measures the heterogeneity of the micellar interface. The obtained values $\gamma \simeq 0.3-0.35$ and $\gamma \simeq 0.6$ (see Tab. 1) estimate the different complexity of the $C_{12}E_6$ and LDAO interfaces, respectively.

V. Rotational Relaxation

We consider now the rotational diffusion of interfacial waters. For each simulated temperature, we find that the fast decay of $P_1(t)$ and $P_2(t)$ ($t < 50$ ps) is well described by stretched exponentials. Their average relaxation times $< \tau_R^1 >$ and $< \tau_R^2 >$ are reported in Table 2. We first point out that the rotational diffusion of water on the $C_{12}E_6$ micellar surface shows a strong retardation with respect to the bulk relaxation, with $< \tau_R^1 > = 140$ ps at $T = 10$ °C and $< \tau_R^1 > = 54.3$ ps at $T = 45$ °C. This compares with the first-rank relaxation time for bulk water of ∼1.9−3.7 ps depending on the water model potential and temperature (see Table 2).

In Figure 3 we compare our results for $P_2(t)$ obtained from simulation of the two micelles and two models of bulk water, TIP3P and SPC, simulated at the same thermodynamics condition of the micellar solutions. This clearly shows that the dynamics of hydration water for LDAO is much closer to that of the bulk (panel C) than in the case of $C_{12}E_6$ (panels A and B). As in the case of the survival probability $N_w(t)$, the stretched decay of the dipolar relaxations mirrors the complexity of the energetic landscape for the dipolar rotation. For the $C_{12}E_6$ micelle the γ exponent is about 0.3−0.4 depending on the dipolar rank whereas for LDAO $\gamma = 0.66$ and 0.68. Thus it is reproduced the trend observed for the stretched decay of the survival probability $N_w(t)$.

We now turn our attention to the ratio r between the first and second rank average relaxation time defined in eq 6. This is close to 3 for an isotropic diffusion model of the hydration waters. Remarkably, $C_{12}E_6$ shows a strong deviation from this model as r is here close to 1 at both the temperatures we have studied. This result shows that the rotation of water molecules is constrained in an anisotropic space. Indeed, the long hydrophilic heads form strong hydrogen bonds with water,[23] thus creating a trapping environment for water. A similar deviation from the isotropic rotational diffusion model has also been found for low hydrated PEO/Water solutions.[44]

In contrast, the lack of possible water confinement site at the LDAO/water interface makes the rotational diffusion of the hydration layer much more like that of the bulk. In this case we find a value of r close to 3, i.e., $r = 3.6$.

VI. Translational Diffusion

The mean square displacement (MSD), or $< |\mathbf{r}(t) - \mathbf{r}(0)|^2 >$, for water molecules in the hydration shell of the $C_{12}E_6$ micelle at $T = 45$ °C is shown in panel A) of Figure 4 and compared with bulk SPC water at the same thermodynamic conditions. First we remark that the MSD of hydration water in this micelle follows a power law rather than a linear dependence in time as that observed for bulk water. A similar behavior is also observed at $T = 10$ °C. In both cases we find the MSD obeying the law:

$$\langle |\mathbf{r}(t) - \mathbf{r}(0)|^2 \rangle \propto t^{\alpha} \tag{7}$$

Our fit gives $\alpha = 0.3$ at $T = 10$ °C and $\alpha = 0.4$ at $T = 45$ °C, an $\alpha < 1$ denoting a dispersive diffusion. This sub-diffusive dynamics has already been observed for water on protein surfaces, although with larger values of α, $\alpha \simeq 0.6$,[2,9] and in other micellar systems.[19] This behavior is generally assumed to be a consequence of the geometric and/or energetic disorder experienced by water on a biological surface.[10]

As in a previous paper,[9] to extract the residence times we follow the NMRD experimental estimates and define it as the time required by a water molecules to cover 3 Å, i.e., the diameter of a water molecule. Thus, at $T = 10$ °C we extrapolate a residence time of $\tau_w \simeq 500$ ps, whereas at $T = 45$ °C we find $\tau_w \simeq 70$ ps. It's interesting to point out that at the lower temperature, the residence times estimated from rotational ($\tau_R^1 = 140$ ps) and translational ($\tau_w = 500$ ps) diffusion strongly differ. Thus, the energetic barrier for rotation and translation on the micellar surface are very different. This difference is less marked at higher temperatures.

In the proximity of the LDAO surface, water behaves more like bulk water, the MSD of the hydration water is close to be linear in time, see panel B) of Figure 4. Thus, we find a larger α, i.e., $\alpha = 0.85$, and a smaller residence time of $\tau_w = 3.2$ ps, not far from $\tau = 2.6$ ps obtained for bulk TIP3P water. For the LDAO micelle, at variance with our findings for a $C_{12}E_6$ micelle, very similar residence time are obtained from translational and

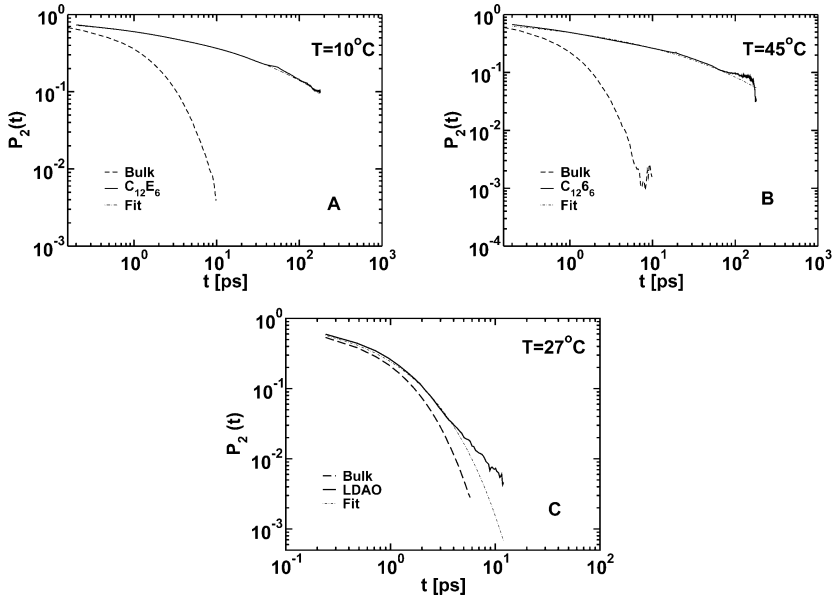

Figure 3. Panels A and B: log−log plot of the second-rank rotational correlation functions computed for a pure water solution (SPC) and for the hydration water molecules in the $C_{12}E_6$ system at $T = 10°$ (panel A) and $T = 45$ °C (panel B) Panel C: log−log plot of the second-rank rotational correlation functions computed for a pure water solution (TIP3P) (bulk) and for hydration water molecules in the LDAO system (LDAO). In all the panels the fitting curves for the hydration water are in dot−dashed lines.

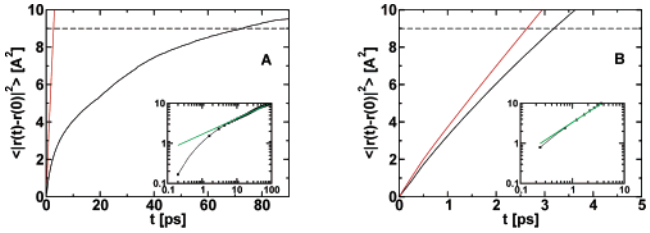

Figure 4. Panel A: Mean square displacement for waters attached to the $C_{12}E_6$ micelle (black) and for bulk SPC water (red) at $T = 45$ °C. The reference distance MSD = 9 Å^2 is plotted as a dashed line. In the inset, the power low fit (green) of the MSD function is shown in a log−log plot. Panel B shows the same results for LDAO.

rotational relaxations calculations. As for the case of a protein some of us investigated in the past, for LDAO the relations $\tau_w \simeq \tau_R^1$ and $r = \tau_R^1/\tau_R^2 \simeq 3$ are satisfied.

Thus, the assumption that the mechanism of translation and rotation of water are rate limited by H-bond disruption, widely used in interpreting NMRD experiments, is correct only for the LDAO micelle. This is not the case for waters trapped in the extended hydrophilic chain of $C_{12}E_6$ system, for which $r \simeq 1$.

VII. Discussion and Conclusion

This paper has provided a quantitative picture of the dynamics of the hydration water near two micelles composed of $C_{12}E_6$ and LDAO surfactants. The two systems strongly differ in the structure of their interface: That of the $C_{12}E_6$ micelle has a higher concentration of large and polar headgroups; on the contrary, that of LDAO has a much larger hydrophobic character with smaller headgroups. Also important is the thickness of the interfacial region, larger for $C_{12}E_6$ than for LDAO due to the large size of the E_6 heads.

We have estimated the residence time of a water molecule near the micelle surface and its retardation with respect to the bulk. Our results show that the water dynamics for the two micellar systems is radically different. In $C_{12}E_6$ at $T = 45°$ C the residence time estimated from dipole−dipole correlations and translational diffusion is 54 and 70 ps. At lower temperature, $T = 10°$ C, its value increases to about 140 and 500 ps, respectively. Thus, surface water dynamics is 1−2 orders of magnitude slower than in the bulk. On the contrary, the residence time for water attachment to the LDAO surface is much smaller and within 18% of that of bulk water.

We find that diffusion of water on the $C_{12}E_6$ surface shows a dispersive diffusion regime described by eq 7 with $\alpha \simeq 0.3-0.4$, whereas for LDAO $< |\mathbf{r}(t) - \mathbf{r}(0)|^2 >$ is closer to linearity. These differences must be traced back to the amount of water strongly bound to the micelle: In $C_{12}E_6$, ≃80% of superficial water is in contact with the hydrophilic moieties and ≃30% forms strong H−Bonds with the solute, whereas on the LDAO surface the majority of water is in contact with the hydrophobic groups exposed to the solvent or forms H-bonds.

Our simulations also reveal the nature of the rotational landscape experienced by water on the micellar surface. In $C_{12}E_6$ micelle water rotation occurs in a highly anisotropic space ($r = 1.33$ at 45 °C and 1.18 at 10 °C), whereas in LDAO the rotational landscape is isotropic ($r = 3.6$). The small r's in $C_{12}E_6$ are a consequence of water confinement at the thick water/micelle interface. In this system, an increase in the temperature produces an increase of the r ratio and signal a weakening of the confinement. Indeed, we find that the number of permanently (i.e., within our simulation time!) attached water molecules decreases of about the 50%. Also, τ_w derived from rotational relaxation and diffusion deviate less than 30% at the lower temperature.

In a seminal paper on water dynamics near biological surfaces, Zewail and co-workers[1] explored the dynamic of hydration around a protein and a micelle at $T = 27$ °C by spectroscopical means. The relaxation of the solvent around a chemical probe showed a slow component in the order of 38 ps for the protein, a subtilisin *Carlsberg*, and of 60 ps for a TX-100 micellar system. Even though the relation between the dielectric response of water, probed by the electronic excitation response experiments and the water residence time is far from clear,[11] our simulation results follow the general trend obtained by femtosecond experiments for their relaxation times. Indeed, in previous papers on hydrated lysozyme at $T = 27$ °C, some of us estimated the water residence time on a protein surface at

$\sim$10−20 ps,[9,43] whereas here we obtain a residence time in the order of 50−70 ps for the micelle $C_{12}E_6$ at $T = 45$ °C. The similarity of the hydrophilic moieties of TX-100 and $C_{12}E_6$ surfactants adds extra leverage to our results.

To conclude, our investigation has shown clearly that the slowdown of interfacial water relaxation near complex micelles depends, case by case, on the structural properties of the interface itself, such as the ratio between hydrophobic/hydrophilic exposed regions and on the interface thickness and topography.

Supporting Information Available: Preparation and equilibrium of the $C_{12}E_6$ and force field for LDAO. This material is available free of charge via the Internet at http://pubs.acs.org.

References and Notes

(1) Pal, S.; Peon, J.; Zewail, A. H. *Proc. Natl. Acad. Sci. U.S.A.* **2002**, *99* (4), 1763.

(2) Bizzarri, A. R.; Cannistraro, S. *J. Phys. Chem B* **2002**, *106*, 6617−6633.

(3) Sen, P.; Mukherjee, S.; Dutta, P.; Halder, A.; Mandal, D.; Banerjee, R.; Roy, S.; Bhattacharyya, K. *J. Phys. Chem B* **2003**, *107*, 14563−14568.

(4) Pal, S.; Peon, J.; Bagchi, B.; Zewail, A. H. *J. Phys. Chem B* **2002**, *106*, 12376−12395.

(5) Pal, S.; Zhao, L.; Zewail, A. H. *Proc. Natl. Acad. Sci. U.S.A.* **2003**, *100*, 8113−8118.

(6) Datta, A.; Mandal, D.; Pal, S. K.; Bhattacharyya, K. *J. Mol. Liq.* **1998**, *77*, 121.

(7) Balasubramanian, S.; Bagchi, B. *J. Phys. Chem. B* **2001**, *105*, 12529.

(8) Senapati, S.; Berkowitz, M. L. *J. Chem. Phys.* **2003**, *118*, 1937−1941.

(9) Marchi, M.; Sterpone, F.; Ceccarelli, M. *J. Am. Chem. Soc.* **2002**, *124*, 6787.

(10) Rocchi, C.; Bizzarri, A. R.; Cannistraro, S. *Phys. Rev. E* **1998**, *57*, 3315.

(11) L.Nilsson; Halle, B. *Proc. Natl. Acad. Sci. U.S.A.* **2005**, *102*, 13867−13872.

(12) Halle, B. In *Hydration Process in Biology;* Bellissent-Funel, M. C., Et.; IOS Press: Ohmsha, 1999.

(13) Sarkar, N.; Datta, A.; Das, S.; Bhattacharyya, K. *J. Phys. Chem* **1996**, *100*, 15483.

(14) Jordanides, X. J.; Lang, M. J.; Song, X.; Fleming, G. R. *J. Phys. Chem* **1999**, *103*, 7995.

(15) Kumbhar, M.; Goel, T.; Mukherjee, T.; Pal, H. *J. Phys. Chem B* **2004**, *108* (4), 19246−19254.

(16) Vass, S.; Grimm, H.; Bányai, I.; Meier, G.; Gilányi, T. *J. Phys. Chem B* **2005**, *109*, 11870.

(17) Balasubramanian, S.; Bagchi, B. *J. Phys. Chem. B* **2002**, *106*, 3668.

(18) Pal, S.; Balasubramanian, S.; B. Bagchi. *J. Chem. Phys.* **2002**, *117*, 2852.

(19) Balasubramanian, S.; Pal, S.; Bagchi, B. *Phys. Rev. Lett.* **2002**, *89* (11), 115505.

(20) Bruce, C. D.; Senapati, S.; Berkowitz, M. L.; Perera, L.; Forbes, M. D. E. *J. Phys. Chem. B* **2002**, *106*, 10902−10907.

(21) Sterpone, F.; Pierleoni, C.; Brigonti, G.; Marchi, M. *Langmuir* **2004**, *20*, 4311−4314.

(22) Puvvada, S.; Blankschtein, D. *J. Chem. Phys.* **1990**, *92*, 3710.

(23) Tasaki, K. *J. Am. Chem. Soc.* **1996**, *118*, 8459.

(24) Sterpone, F.; Briganti, G.; Pierleoni, C. *Langmuir* **2001**, *17*, 5103.

(25) Berendsen, H. J. C.; Postma, J. P. M.; vanGunsteren, W. F.; Hermans, J. In *Intermolecular Forces;* Pullman, B., Ed.; Reidel Publishing Company: Dordrecht, The Netherlands, 1981.

(26) Ryckaert, J. P.; Ciccotti, G.; Berendsen, H. J. C. *J. Comput. Phys.* **1977**, *23*, 327.

(27) Essmann, U.; Perera, L.; Berkowitz, M. L.; Darden, T.; Lee, H.; Pedersen, L. G. *J. Chem. Phys.* **1995**, *103*, 8577.

(28) Melchionna, S.; Ciccotti, G. *J. Chem. Phys.* **1997**, *106*, 195.

(29) S. Melchionna; S. Cozzini. *DLPROTEIN user manual: 2001;* University of Rome.

(30) Barlow D. J.; Lawrence M. J.; Zuberi T.; Zuberi S.; Heenan R. K. *Langmuir* **2000**, *16*, 10398.

(31) MacKerell-Jr., A.; Bashford, D.; Bellot, M.; Dunbrack-Jr., R.; Evanseck, J.; Field, M.; Fischer, S.; Gao, J.; Guo, H.; Ha, S.; Joseph-McCarthy, D.; Kuchnir, L.; Kuczera, K.; Lau, F.; Mattos, C.; Michnick, S.; Ngo, T.; Nguyen, D.; Prodhom, B.; III, W. R.; Roux, B.; Schlenkrich, M.; Smith, J.; Stote, R.; Straub, J.; Watanabe, M.; Wiorkiewicz-kuczera, J.; Yin, D.; Karplus, M. *J. Phys. Chem B* **1998**, *102*, 3586−3616.

(32) Ceccarelli, M.; Procacci, P.; Marchi, M. *J. Comput. Chem.* **2003**, *24*, 129.

(33) Jorgensen, W. L.; Chandrasekhar, J.; Madura, J. D.; Impey, R. W.; Klein, M. L. *J. Chem. Phys.* **1983**, *79*, 926.

(34) Marchi, M.; Procacci, P. *J. Chem. Phys.* **1998**, *109*, 5194−5202.

(35) Procacci, P.; Darden, T. A.; Paci, E.; Marchi, M. *J. Comput. Chem.* **1997**, *18*, 1848−1862.

(36) Procacci, P.; Marchi, M. In *Advances in the Computer Simulations of Liquid Crystals*, Proceedings of the NATO-ASI School, Erice 11−21 June 1998; Zannoni, C., Pasini, P., Eds; Kluwer Academic: Dodrecht, The Netherlands, 1999.

(37) Voronoi, G. F. *J. Reine Angew. Math* **1908**, *134*, 198−287.

(38) Procacci, P.; Scateni, R. *Int. J. Quantum Chem.* **1992**, *42*, 1515−1528.

(39) Impey, R. W.; Madden, P. A.; McDonald, I. *J. Phys. Chem.* **1983**, *87*, 5071−5083.

(40) Allen, R.; Bandyopadhyay, S.; Klein, M. L. *Langmuir* **2000**, *16*, 10547.

(41) Romsted, L. S.; Yao, J. *Langmuir* **1996**, *12*, 2425−2432.

(42) Abel, S.; Sterpone, F.; Bandyopadhyay, S.; Marchi M. *J. Phys. Chem. B* **2004**, *108*, 19458−19466.

(43) Sterpone, F.; Marchi, M.; Ceccarelli, M. *J. Mol. Biol.* **2001**, *311*, 409−419.

(44) Borodin, O.; Bedrov, D.; Smith, G. *J. Phys. Chem B* **2002**, *106*, 5194−5199.